EJN European Journal of Neuroscience

FENS Federation of European Neuroscience Societies

European Journal of Neuroscience, Vol. 43, pp. 1474–1485, 2016 doi:10.1111/ejn.13228

MOLECULAR AND SYNAPTIC MECHANISMS

Targeted activation of primitive neural stem cells in the mouse brain

Rachel L. Reeve,[1] Samantha Z. Yammine,[2] Brian DeVeale[2] and Derek van der Kooy[1,2]
[1]Institute of Medical Science, University of Toronto, 160 College St. W. 1130, Toronto, ON, Canada
[2]Department of Molecular Genetics, University of Toronto, Toronto, ON, Canada

Keywords: cell surface markers, endogenous activation, gene expression, neurogenesis

Edited by Paul Bolam
Received 14 January 2015, revised 14 May 2015, accepted 29 February 2016

Abstract

Primitive neural stem cells (pNSCs) are the earliest NSCs to appear in the developing forebrain. They persist into the adult forebrain where they can generate all cells in the neural lineage and therefore hold great potential for brain regeneration. Thus, pNSCs are an ideal population to target to promote endogenous NSC activation. pNSCs can be isolated from the periventricular region as leukaemia inhibitory factor-responsive cells, and comprise a rare population in the adult mouse brain. We hypothesized that the pup periventricular region gives rise to more clonal pNSC-derived neurospheres but that pup-derived pNSCs are otherwise comparable to adult-derived pNSCs, and can be used to identify selective markers and activators of endogenous pNSCs. We tested the self-renewal ability, differentiation capacity and gene expression profile of pup-derived pNSCs and found them each to be comparable to adult-derived pNSCs, including being GFAP^{-}, nestin^{mid}, Oct4^{+}. Next, we used pup pNSCs to test pharmacological compounds to activate pNSCs to promote endogenous brain repair. We hypothesized that pNSCs could be activated by targeting the cell surface proteins C-Kit and ErbB2, which were enriched in pNSCs relative to definitive NSCs (dNSCs) in an *in vitro* screen. C-Kit and ErbB2 signalling inhibition had distinct effects on pNSCs and dNSCs *in vitro*, and when infused directly into the adult brain *in vivo*. Targeted activation of pNSCs with C-Kit and ErbB2 modulation is a valuable strategy to activate the earliest cell in the neural lineage to contribute to endogenous brain regeneration.

Introduction

Identifying cell type-specific markers is a key goal in neural stem cell (NSC) biology. The lack of selective cell markers currently limits efforts to isolate pure cell populations or test selective pharmacological interventions (Obermair *et al.*, 2010; Miller & Kaplan, 2012), a problem that is magnified in rare cell populations. Primitive NSCs (pNSCs) are LIF-dependent, express Oct4 and arise at day 5.5 of mouse embryonic development in advance of definitive NSCs (dNSCs) that arise at embryonic day 7.5 (Hitoshi *et al.*, 2004; Akamatsu *et al.*, 2009). Adult pNSCs are rare Oct4^{+} cells in the adult forebrain periventricular region that arise first in the NSC lineage and give rise to dNSCs and downstream neuronal and glial progenitors (Sachewsky *et al.*, 2014). pNSCs produce clonal LIF-dependent neurospheres in culture that can be passaged to self-renew or give rise to glial fibrillary acidic protein-positive (GFAP^{+}) dNSCs (also termed type B cells) that generate epidermal growth factor (EGF)- and fibroblast growth factor (FGF)-dependent neurospheres (Doetsch *et al.*, 1999; Morshead *et al.*, 2003). pNSCs and dNSCs are cultured in separate culture conditions (LIF or EGF/FGF, respectively) and give rise to clonal neurospheres when cultured at low density and not disturbed during the incubation period (Coles-Takabe *et al.*, 2008).

Despite the lifelong presence of NSCs, the brain exhibits limited endogenous repair to counteract neurodegenerative disease or heal after injury. Pharmacological compounds to activate endogenous NSCs and guide their differentiation could improve brain recovery/repair (Miller & Kaplan, 2012). Therapeutic benefit might be achieved by activating pNSCs to lead to large expansion of dNSCs and their progeny from the top of the neural lineage, which could then be guided to differentiate into needed cell types. We identified pNSC-specific cell surface markers and tested candidate pNSC-mediators on the relatively abundant pup population to identify activators of endogenous adult pNSCs. We demonstrate that pup-derived pNSCs are a valid model for discovering activators of rare adult pNSCs.

A previous mass spectrometry-based screen identified cell surface proteins expressed on embryonic stem cell (ESC)-derived pNSCs (DeVeale *et al.*, 2014). *In vitro*, pNSCs arise from ESCs passaged into serum-free culture conditions containing LIF and proliferate to generate clonal primitive neurospheres (Tropepe *et al.*, 2001). C-Kit and ErbB2 were upregulated on pNSCs relative to upstream ESCs and downstream dNSCs (DeVeale *et al.*, 2014). C-kit is expressed in the olfactory bulbs, hippocampus and cortex in the adult mouse

Correspondence: Dr R. L. Reeve, as above.
E-mail: rachel.leeder@utoronto.ca

brain and on neural progenitors in culture (Motro *et al.*, 1991; Erlandsson *et al.*, 2004). C-kit is a tyrosine kinase receptor that is activated by Steel, mast cell growth factor and stem cell factor (SCF), and activates PI3-kinase, STAT and RAS/MAPK pathways (Keshet *et al.*, 1991; Motro *et al.*, 1991; Blom *et al.*, 2008). ErbB2 is an EGF-R family member that is expressed in the periventricular region and cortex of the adult mouse brain (Fox & Kornblum, 2005). Activation of the ErbB2 receptor preferentially targets Ras/MAPK and to a lesser extent PI3-kinase (Yarden & Sliwkowski, 2001). Our validation of these cell surface proteins as effective modulators of pNSCs makes them ideal candidates for future targeted therapies.

Materials and methods

Mouse strains

Oct4-GFP mice were a kind gift from Dr A. Nagy (Viswanathan *et al.*, 2003). Nestin-GFP mice were a kind gift from Dr G. Enikolopov (Mignone *et al.*, 2004). GFAP-GFP mice were purchased from Jackson (Bar Harbor, ME, USA; #010835). CD1 mice were purchased from Charles River (Wilmington, MA, USA). Mice were used at 8–12 weeks of age. All mice were maintained in the Department of Comparative Medicine, University of Toronto, in accordance with the Guide to the Care and Use of Experimental Animals and approved by the Animal Care Committee.

Primary dissections and neurosphere cultures

The neurosphere assay was performed as previously described (Chiasson *et al.*, 1999). Mice were killed by cervical dislocation, brains were removed and lateral ventricle walls were dissected. Cells were plated at clonal density of 10 cells/μL (Coles-Takabe *et al.*, 2008) in 24-well culture plates (Nunclon; Thermo Scientific, Waltham, MA, USA). Primitive neurospheres were plated in serum-free media (SFM) (Tropepe *et al.*, 1999), supplemented with leukaemia inhibitory factor (LIF, 10 ng/mL). Definitive neurospheres were grown in SFM supplemented with EGF (20 ng/mL; Sigma, St Louis, MO, USA), basic FGF (10 ng/mL; Sigma) and heparin (2 μg/mL; Sigma). Neurospheres were counted after 7–10 days *in vitro*. Primitive neurospheres are > 50 μm and definitive neurospheres are > 100 μm in diameter; these cell populations are cultured separately.

Pharmacological inhibitors dissolved in DMSO and siRNAs were added to the cell culture media at the time of plating. Gleevec (a form of Imatinib), a C-Kit signalling inhibitor (Toronto Research Chemicals, Toronto, Canada; G407000), SCF, a C-Kit ligand (R&D Systems, Minneapolis, MN, USA; 455-MC) and an ErbB2 inhibitor (VWR, Radnor, PA, USA; CA95061-882) were used at varying doses. Smart pool siRNAs included GAPD siRNA as a positive control (Dharmacon, Lafayette, CO, USA; ON-TARGETplus GAPD, D-001830-20-05), C-Kit siRNA (Dharmacon, ON-TARGETplus Kit siRNA, LU-042174-00), ErbB2 siRNA (Dharmacon, ON-TARGETplus ErbB2, LU-064147-00) and scramble siRNA (Dharmacon, ON-TARGETplus Non-targeting siRNA #1, D-001810-01) were transfected using DharmaFECT 1 Transfection (Dharmacon). GAPD siRNA served as a positive control for the knockdown and scramble siRNA as a negative control.

Neurosphere differentiation

After 7 days in culture, neurospheres were individually picked and plated onto Matrigel-coated plates (4% Matrigel in SFM, Sigma). Spheres were differentiated for 7 days in the presence of 1% fetal bovine serum (Life Technologies, Carlsbad, CA, USA), and fixed in 4% paraformaldehyde (PFA) (Sigma) at room temperature.

Stem cell self-renewal assay

To test for self-renewal, individual neurospheres were picked, transferred to an Eppendorf tube containing 200 μL SFM with growth factors, triturated 30–50 times with a pipette tip, and transferred into an additional 300 μL of media in a 24-well plate. The number of secondary neurospheres per primary neurosphere was counted after 7–10 days *in vitro*.

Immunostaining and imaging

Wholemounts were performed as previously described (Mirzadeh *et al.*, 2008). Briefly, brains were dissected to expose the lateral ventricle and fixed overnight in 4% PFA at 4 °C. Wholemounts were washed, immunohistochemistry was performed, and they were then dissected and the lateral ventricle wall was placed onto a microscope slide with aquamount and a coverslip.

Fixed cells were stored in St-PBS at 4 °C. Cell cultures were permeabilized with 0.3% Triton-X in PBS for 5 min at room temperature for internal proteins. Samples were blocked with 10% NGS (normal goat serum, Jackson Labs) in St-PBS (with 2% Triton X-100 for wholemounts) for 1 h at room temperature. Primary antibodies were diluted in blocking solution at 4 °C overnight for plated cells and 48 h for wholemounts. Secondary antibodies were incubated again in blocking solution for 40 min at room temperature for differentiated spheres and 48 h at 4 °C for wholemounts. Nuclei were counterstained with Hoechst (1 : 1000, Sigma).

The primary antibodies were rabbit anti-GFAP (Sigma, G9269, 1 : 400), mouse anti-O4 (Millipore, Billerica, MA, USA, MAB345, 1 : 200), rabbit anti-GFAP (Sigma, G9269, 1 : 400), mouse anti-βIII tubulin (Sigma, T8660, 1 : 400), chicken anti-GFP (Aves Lab, Tagard, OR, USA, GFP-1020, 1 : 500), rabbit anti-SOX2 (Abcam, Cambridge, MA, USA, ab97959, 1 : 500), rabbit anti-β-catenin (Sigma, C2206, 1 : 500), rabbit anti-LIF-R (Abcam, ab101228, 1 : 500), rabbit anti-c-kit (Abcam, ab5506) and mouse anti-ErbB2 (Abcam, ab16901). Secondary antibodies included: 488 goat anti-chicken (Alexa, A11039, 1 : 400), 488 goat anti-mouse (Alexa, A11029, 1 : 400), 488 goat anti-rabbit (Alexa, A11034, 1 : 400), 568 goat anti-mouse (Alexa, A11031, 1 : 400) and 568 goat anti-rabbit (Alexa, A11036, 1 : 400). Nuclei were stained with Hoescht (Sigma, 33258, 1 : 1000). Staining was visualized on an AxioVision Zeiss UV microscope and Nikon 200 microscope or Olympus Fluoview FV1000 confocal laser scanning microscope.

Quantitative PCR

ESCs, ESC-derived pNSCs, pNSC pup- and adult-derived colonies, pNSC pup-derived neurospheres, and dNSC pup- and adult-derived neurospheres were collected in buffer RLT with β-mercaptoethanol. RNA was extracted using the RNeasy Micro Kit (Qiagen, Valencia, CA, USA), including treatment with the RNase-free DNase Set (Qiagen). cDNA was synthesized with a Superscript III First Strand Synthesis System (Invitrogen, Carlsbad, CA, USA). qPCR was performed on a 7900HT Fast Real-Time PCR System (Applied Biosystems, Foster City, CA, USA). Cycling conditions were: 2 min at 50 °C, 10 min at 95 °C, followed by 40 cycles of 15 s at 95 °C, 1 min at 60 °C and 15 s at 95 °C. Ct values were normalized to GAPDH and expressed relative to ESCs. The Taqman probes used

were: GAPDH (Mm03302249_g1), 18S (Mm03928990_g1), Oct4/Pou5fl (Mm03053917_g1), Sox2 (Mm03053810_s1), Klf4 (Mm00516104_m1), Nanog (Mm02019550_s1), Mash1/Ascl1 (Mm03058063_m1), Nestin (Mm00450205_m1), Sox1 (Mm00486299_s1), c-kit (Mm00445212_m1 kit) and ErbB2 (Mm00658541_m1 ErbB2) (ThermoFisher, Waltham, MA, USA).

Fluorescence-activated cell sorting (FACS)

Cells were isolated from primary dissections of Oct4-GFP, GFAP-GFP and nestin-GFP mice for FACS analysis using a FacsAria (BD Biosciences, Franklin Lakes, NJ, USA). Cells were counterstained with propidium iodide (2.5 μg/μL, BD Biosciences) to assess viability and exclude dead cells. CD1 mice were used as negative control and actin-GFP mice were used as positive control to set analysis gates.

Intracerebral infusion

CD1 mice were anaesthetized with 3–5% isoflurane and injected with ketoprofen (3 mg/kg). A cannula was implanted into the lateral ventricle (+0.2 mm anterior, +0.8 mm lateral, and depth of 2.5 mm below the skull, relative to bregma) and connected to a micro-osmotic pump placed subcutaneously on the back (Alzet 1003D, Direct Corp.). Mice received a 3-day infusion of 400 μM C-Kit Inhibitor (Toronto Research Chemicals) or 130 μM ErbB2 Inhibitor (VWR) delivered at 1 μL/h. For flow analysis, mice were killed immediately following intracerebral infusion and cells were prepared for flow analysis by dissection, dissociated with trypsin and resuspended in Hank's balanced saline solution with 10% fetal bovine serum for sorting.

Statistics

Data are represented as means ± SEM unless otherwise stated and as biological replicates. Statistical analyses were performed using GraphPad Prism 5 (GraphPad Software, Inc., La Jolla, CA, USA) and Microsoft Excel. ANOVA with Bonferroni's multiple comparison tests and Student's *t*-test were performed with a significance level of 0.05. Only significant differences of interest are indicated.

Results

Pup-derived pNSCs have similar stem cell properties and gene expression as adult-derived pNSCs

Primary dissections of P7 pup brains generated 30-fold more pNSC neurospheres than 8–12-week adult brain dissections, 1.3 ± 0.2 (mean ± SEM) adult-derived neurospheres vs. 43 ± 3 (mean ± SEM) pup-derived neurospheres per 40 000 cells plated. The pup periventricular region dissection yielded twice as many cells as the adult periventricular region, and therefore on an absolute basis the pup brain generates greater than 60-fold more pNSCs neurospheres than the adult brain. This increase in prevalence suggested pup-derived pNSCs would be ideal for drug screening and validation, as long as they shared similar properties to adult pNSCs. To confirm that pup-derived pNSCs are equivalent to adult-derived pNSCs, we compared morphology, self-renewal, differentiation and gene expression between the two populations. Similar to adult-derived pNSCs (Sachewsky *et al.*, 2014), P7 pup-derived pNSCs formed clonal, LIF-dependent, free-floating neurospheres > 50 μm in diameter with clearly defined borders, while P7 pup-derived dNSCs neurospheres were EGF- and FGF-dependent and > 100 μm in diameter (Fig. 1A). Single sphere passaging demonstrated that pup- and adult-derived clonal pNSC colonies self-renewed at the same frequency, 0.44 ± 0.03 (mean ± SEM) per pup neurosphere passaged vs. 0.38 ± 0.06 (mean ± SEM) per adult neurosphere passaged (Chi-square $P = 0.52$). The self-renewal ability indicates the same frequency of stem cells in pup- and adult-derived pNSC colonies.

We confirmed that pup-derived pNSCs are multipotent and that clonal neurospheres gave rise to neurons, astrocytes and oligodendrocytes in culture (Fig. 1B). Similar to adult-derived pNSCs (Sachewsky *et al.*, 2014), pup-derived pNSCs produced significantly fewer $GFAP^+$ astrocytes than adult- and pup-derived dNSCs and their differentiation profile was markedly different from pup-derived dNSCs (Fig. 1C and D). Pup-derived pNSCs and dNSCs gave rise to a significantly increased proportion of oligodendrocytes compared to adult-derived pNSCs and dNSCs (Sachewsky *et al.*, 2014). This may reflect a contribution to the wave of oligogenesis that occurs predominantly between postnatal days 7 and 21 during mouse brain development (Sauvageot & Stiles, 2002). Pup pNSC-derived neurospheres gave rise to neurons, astrocytes and oligodendrocytes, confirming that they are a multipotent stem cell population, similar to adult pNSCs.

Next, qPCR for pluripotency and neural genes confirmed that pup-derived pNSCs had similar gene expression to adult-derived pNSCs. We compared ESC-derived primitive neurospheres, adult-derived pNSC colonies, and adult-derived and pup-derived pNSCs colonies and neurospheres. Colonies are adherent and grown on a feeder layer in the presence of serum with LIF, and neurospheres are free floating in serum-free media with LIF. Regardless of age of origin, pNSC-derived colonies and neurospheres had higher levels of RNA expression from the pluripotency genes *Oct4*, *Klf4* and *Nanog*, with lower expression from the neural genes *Mash1* and *nestin* compared to dNSC neurospheres (Fig. 1E). pNSCs had lower levels of Sox2 RNA than dNSCs, a gene implicated in stem cell proliferation (Julian *et al.*, 2013; Surzenko *et al.*, 2013), suggesting that pNSCs might have reduced proliferative capacity compared to dNSCs. Pup-derived pNSC neurospheres had increased Sox2 RNA levels, while pup-derived pNSC colonies and spheres had increased Mash1 and Sox1 compared to adult-derived pNSC colonies (Fig. 1E). This reflects age-dependent differences in the pNSC progeny as colonies/neurospheres predominantly consist of progenitors, and suggests that pNSCs may give rise to different progenitors based on developmental stage. The characterization of pup-derived pNSCs confirms that they are comparable to adult-derived pNSCs and their increased abundance makes them a valuable population to study methods of targeting endogenous adult pNSCs.

Pup pNSCs are $Oct4^+$, $Sox2^+$, LIF-R^+, β-$catenin^+$

Adult pNSCs are $Oct4^+$, $SOX2^+$, LIF-R^+, β-$catenin^-$ (Sachewsky *et al.*, 2014), so we investigated whether pup pNSCs express these markers as well. We prepared wholemounts of the lateral ventricle from P7 Oct4-GFP pups to determine whether these proteins are expressed in pup pNSCs (Fig. 2A). In the pup periventricular region, $Oct4^+$ cells were identified that co-localized with SOX2 and LIF-receptor (LIF-R) (Fig. 2B and C). All $Oct4^+$ cells identified were $SOX2^+$ and LIF-R^+; however, the majority of $SOX2^+$ or LIF-R^+ cells were not $Oct4^+$. We previously reported that 80 $Oct4^+$ cells are present in the adult brain (Sachewsky *et al.*, 2014), and thus they comprise a subpopulation of the $SOX2^+$ LIF-R^+ cells. In contrast to adult pNSCs, $Oct4^+$ cells co-expressed β-catenin in the pup brain (Fig. 2D). β-Catenin stained the ventricular surface extensively and labelled fewer cells deeper in the subependymal zone where it

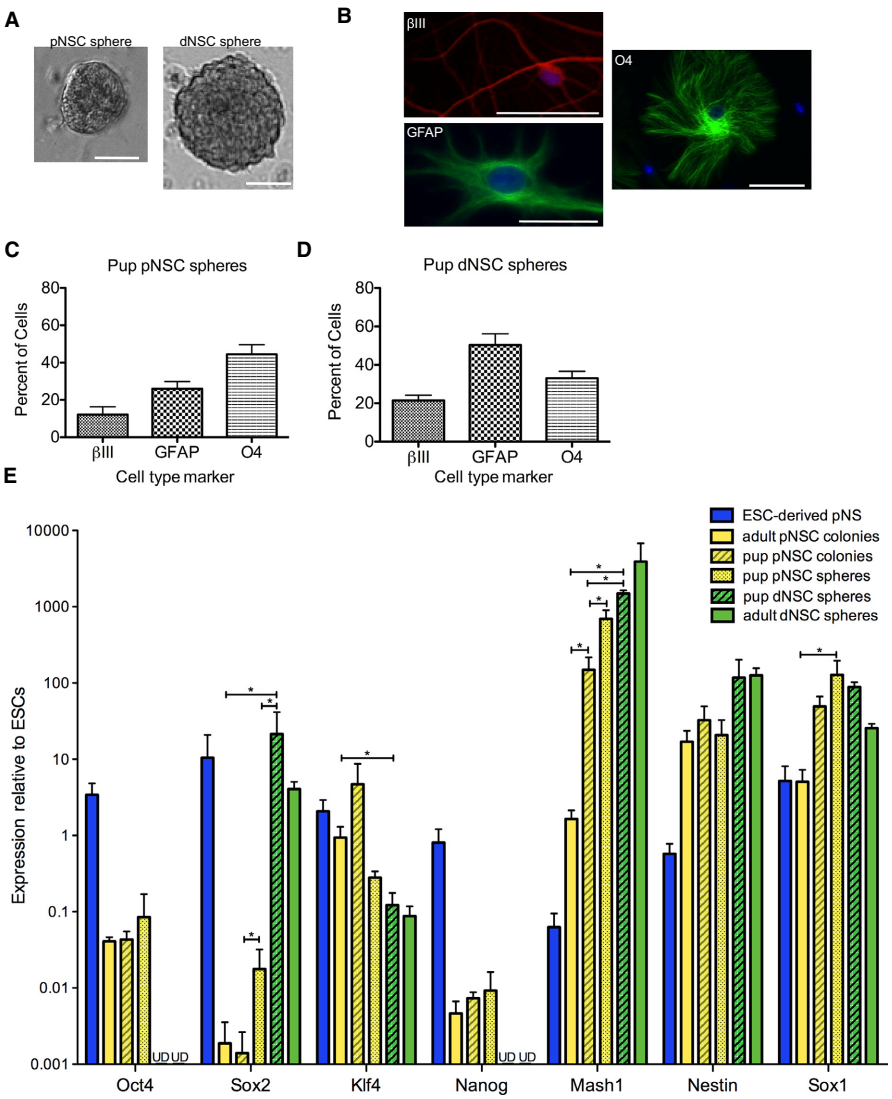

FIG. 1. Characterization of pup-derived pNSCs. (A) Morphology of a clonal pNSC-derived neurosphere and dNSC-derived neurosphere from P7 mouse brain; scale bars = 50 μm. (B) Pup-derived pNSCs differentiate to give rise to βIII$^+$ neurons, GFAP$^+$ astrocytes and O4$^+$ oligodendrocytes. (C) Differentiation profile of pNSC neurospheres derived both postnatal day 7 pups (n = 7–9 neurospheres from three independent experiments). (D) Differentiation profile of pup-derived dNSCs neurospheres (n = 7–10 neurospheres from three independent experiments). dNSC-derived neurospheres give rise to significantly more GFAP$^+$ cells than pNSC-derived neurospheres. In addition, pup-derived pNSC neurospheres and dNSC neurospheres gave rise to significantly more O4$^+$ cells than adult-derived pNSC neurospheres and dNSC neurospheres (two-way ANOVA $F_{6,67}$ = 11.4, P = 0.01, n = 3). (E) Pup- and adult-derived pNSC colonies express similar levels of stem cell and neural genes. qPCR of pNSC colonies/spheres and dNSC spheres is expressed relative to ESCs and normalized to GAPDH. Pup-derived pNSCs express similar levels of the pluripotency factors Oct4, Klf4 and Nanog, equivalent nestin expression, and increased Mash1 and Sox1 mRNA compared to adult-derived pNSCs (two-way ANOVA $F_{30,84}$ = 13.6, P = 0.001, n = 3, only select statistical significances are shown). UD = undetectable. *$P \leq 0.05$.

co-localized with Oct4$^+$ cells. This may indicate a difference between the pup and adult pNSCs, or may have resulted from the fact that β-catenin is membrane bound while *GFP* expression by the *Oct4* promoter is cytoplasmic and thus these were mistakenly thought not to overlap due to their different localization within cells (Sachewsky *et al.*, 2014). Interestingly, Oct4$^+$ cells often resided in close proximity to blood vessels (Fig. 2C and D). Thus, the pup brain contains a population of Oct4$^+$, SOX2$^+$, LIF-R$^+$, β-catenin$^+$ cells in the periventricular region.

pNSCs can be isolated from dNSCs based on Oct4, GFAP and nestin expression

In addition to visualizing Oct4$^+$ pNSCs in the periventricular region to identify protein co-expression based on immunohistochemistry, we performed FACS in conjunction with the neurosphere assay to determine gene expression in sphere-initiating pNSCs. This technique was not successful in adult-derived pNSCs due to their rarity (Sachewsky *et al.*, 2014). First, we confirmed that pup-derived sphere-initiating pNSCs are Oct4$^+$ by performing FACS analysis on primary cells from the periventricular region of Oct4-GFP P7 pups to isolate Oct4$^+$ cells (Fig. 3A). Oct4$^-$ and Oct4$^+$ cells, along with an ungated control, were plated in the neurosphere assay in either EGF/FGF or LIF. pNSC-derived neurospheres arose exclusively from the Oct4$^+$ population at significantly increased frequency over the ungated control, confirming that pNSCs are Oct4$^+$ (Fig. 3B). dNSC-derived neurospheres arose from the Oct4$^-$ population, confirming that dNSCs from the pup brain are Oct4$^-$, like those found in the adult (Fig. 3C). However, fewer dNSCs arose from the Oct4$^-$ population than the ungated control, suggesting that some dNSCs

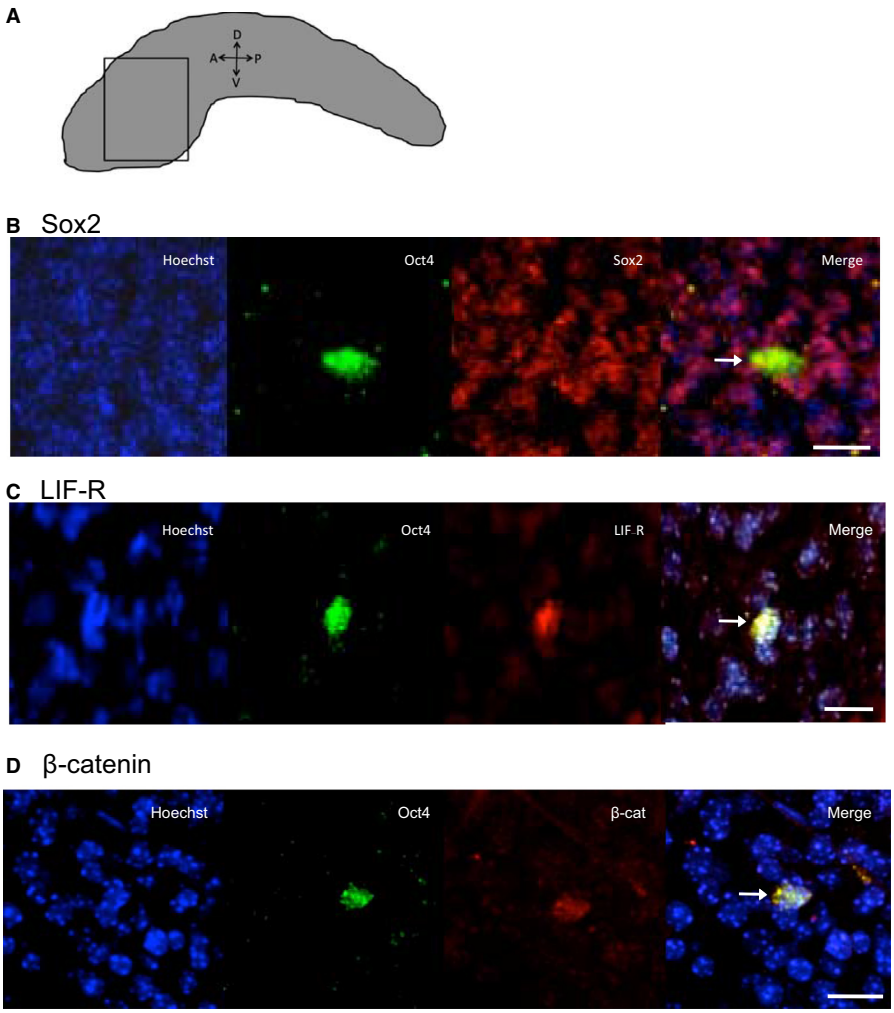

FIG. 2. pNSC markers in the walls of the lateral ventricle. (A) Wholemounts were prepared from Oct4-GFP pups (region imaged is indicated with a box). Wholemounts were stained with anti-GFP and counterstained for (B) Sox2, (C) LIF-R and (D) β-catenin. Scale bars = 10 μm. Arrows indicate cells of interest.

were in the middle unsorted population. We conclude that *Oct4* expression is exclusive to pNSCs and a defining difference from dNSCs in the pup brain.

To further substantiate the claim that neurospheres grown in EGF and FGF arise from GFAP$^+$ dNSCs while those that arise in LIF are from GFAP$^-$ pNSCs, we performed FACS on primary cells from GFAP-GFP mice to isolate GFAP$^-$ and GFAP$^+$ cells (Fig. 3D). We observed that pNSCs are GFAP$^-$ as the number of LIF-dependent neurospheres was significantly increased in the GFAP$^-$ population compared to the ungated control (Fig. 3E). Pup dNSCs were GFAP$^+$ as EGF- and FGF-dependent neurospheres were significantly increased in the GFAP$^+$ population compared to the ungated control (Fig. 3F). The few EGF- and FGF-dependent neurospheres from the GFAP$^-$ population and LIF-dependent neurospheres from the GFAP$^+$ population are probably due to technical constraints, as we gated to maximize viability at the expense of purity. This issue is not observed in the Oct4-GFP or nestin-GFP sorts but may arise in the GFAP-GFP sorts exclusively due to the low level of *GFAP* expression in dNSCs as compared to *GFAP* expression in astrocytes. Together these flow cytometry data confirm previous reports from the adult brain that pNSCs are GFAP$^-$ and that dNSCs that generate neurospheres in EGF and FGF are GFAP$^+$ (Chiasson *et al.*, 1999; Doetsch *et al.*, 1999; Morshead *et al.*, 2003; Sachewsky *et al.*, 2014).

Subsequently, we used the nestin-GFP mouse strain to determine nestin expression in pNSCs. Nestin is commonly described as a neural stem/progenitor marker and is also expressed in many immature and proliferating cells (Gilyarov, 2008). We sought to determine whether nestin is expressed in pNSCs, as it is in dNSCs. We performed primary dissections and isolated cells based on low, middle or high nestin expression (Fig. 3G). pNSC-derived neurospheres arose exclusively from the nestin^{mid} population, a significant increase over the ungated control (Fig. 3H). dNSC-derived neurospheres arose overwhelmingly from the nestin^{high} population, also a significant increase over ungated control (Fig. 3I). This trend of higher *nestin* expression in dNSCs than pNSCs was corroborated by qPCR for both pup and adult populations (Fig. 1F). Therefore, pNSCs and dNSCs have different levels of nestin expression and reduced nestin is a defining feature of pNSCs relative to dNSCs.

Cell surface markers identified on ESC-derived pNSCs target pup-derived pNSCs in vitro

A previous mass spectrometry-based analysis identified novel cell surface markers upregulated on ESC-derived pNSCs compared to ESCs and dNSCs (DeVeale *et al.*, 2014). In this study, C-Kit and ErbB2 receptors were upregulated on ESC-derived pNSCs and their

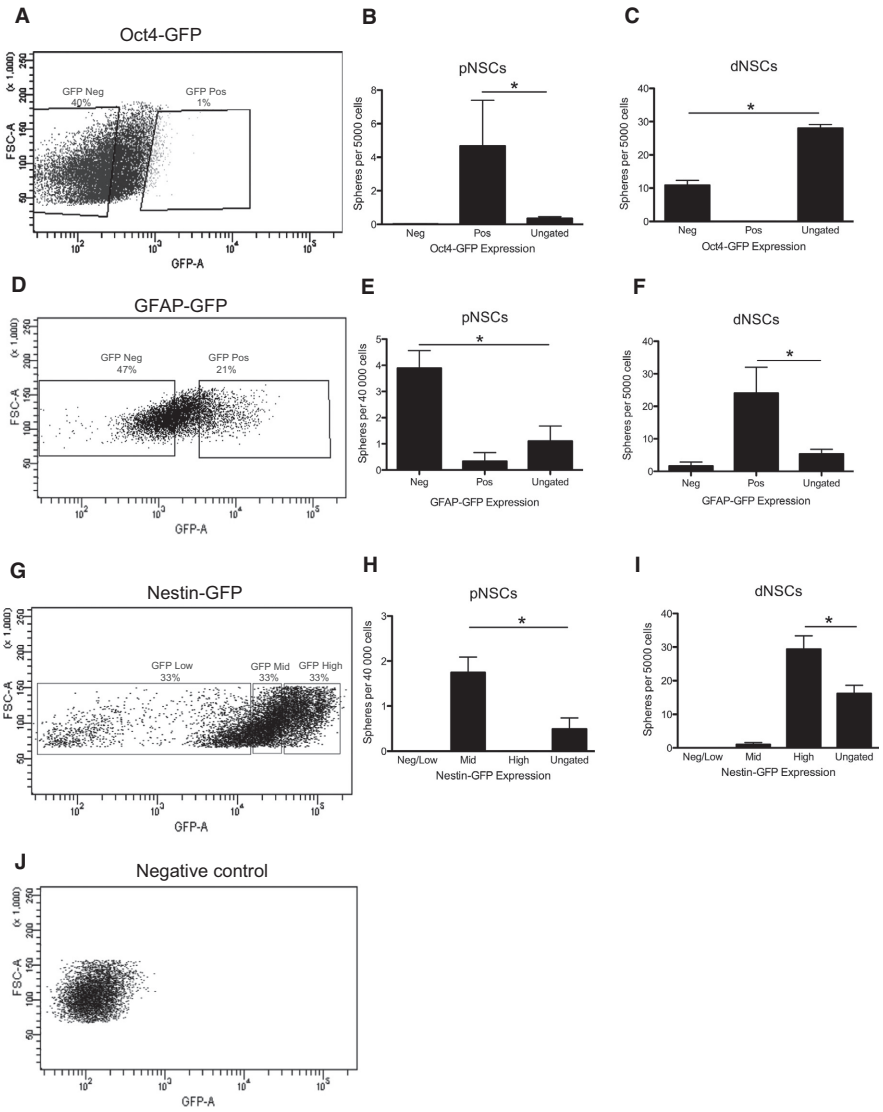

FIG. 3. FACS analysis of primary pup brain cells. (A) Cells from Oct4-GFP pups were sorted to isolate Oct4$^+$ vs. Oct4$^-$ cells. (B) pNSCs arose exclusively from the Oct4$^+$ population, a significant increase over the ungated control (one-way ANOVA $F_{2,6} = 12.53$, $P = 0.01$, $n = 3$). (C) dNSCs arose exclusively from the Oct4$^-$ population (one-way ANOVA $F_{2,6} = 171.4$, $P = 0.001$, $n = 3$). (D) GFAP-GFP periventricular cells were sorted into GFAP$^-$ and GFAP$^+$. (E) pNSCs were significantly enriched in the GFAP$^-$ population (one-way ANOVA $F_{2,6} = 11.55$, $P = 0.01$, $n = 3$). (F) dNSCs were significantly enriched in the GFAP$^+$ population (one-way ANOVA $F_{2,6} = 6.34$, $P = 0.03$, $n = 3$). (G) Nestin-GFP pup cells were sorted for low, middle and high nestin expression. (H) pNSCs arose exclusively from the nestin^{mid} population (one-way ANOVA $F_{3,8} = 15.0$, $P = 0.001$, $n = 3$). (I) dNSCs were significantly increased in the nestin-high population (one-way ANOVA $F_{3,8} = 34.04$, $P = 0.001$, $n = 3$). (J) Negative control of a CD1 mouse. *$P \leq 0.05$.

inhibition affected pNSC-derived neurosphere formation from ESCs. Here, we tested whether the cell surface markers also target pNSCs in primary culture by treating pup-derived pNSCs with pharmacological inhibitors for the C-Kit and ErbB2 receptors and confirmed the specificity of the inhibitors with siRNAs targeted at the corresponding RNAs for either receptor.

To confirm that inhibition of C-Kit increases brain-derived pNSCs, we cultured pup-derived primary cells with C-Kit inhibitor at varying concentrations (Fig. 4A). Gleevec, a C-Kit signalling inhibitor, had a significant interaction effect on pNSCs vs. dNSCs at various concentrations and significantly increased pNSC-derived neurospheres over dNSCs at 4 and 10 μM (Fig. 4B). We confirmed that the Gleevec-mediated increase in pNSCs was C-Kit specific using a Kit siRNA, which decreased C-Kit transcripts to 47% of control (Fig. 4C). Kit siRNA at 100 nM induced a significant increase in pNSCs over the scrambled control, without affecting dNSCs (Fig. 4D). We did not detect a change in neurosphere size in the presence of C-kit siRNA [control pNSC neurospheres were 61 ± 1 μm vs. kit siRNA exposed neurospheres were 62 ± 2 μm (mean ± SEM), $n = 3$]. Primary cells were cultured with the C-Kit ligand SCF at varying concentrations, which depleted pNSC-derived neurospheres and increased dNSC-derived neurospheres (Fig. 4E), the opposite result of Gleevec treatment (Fig. 4B). Next, to test whether C-Kit inhibition was directly affecting the stem/progenitor cells rather than having a secondary effect mediated by niche cells in primary culture, we passaged primary untreated neurospheres into secondary culture with C-Kit inhibitor or C-Kit siRNA (Fig. 4F). The increase in pNSC neurospheres continued in secondary culture and a significant increase over inhibitor-treated dNSCs in the presence of C-Kit inhibitor and C-Kit siRNA (Fig. 4G and H). Neurosphere size was not affected by exposure to C-Kit siRNA (control pNSC neurospheres were 61.6 ± 1.0 μm whereas C-Kit siRNA-

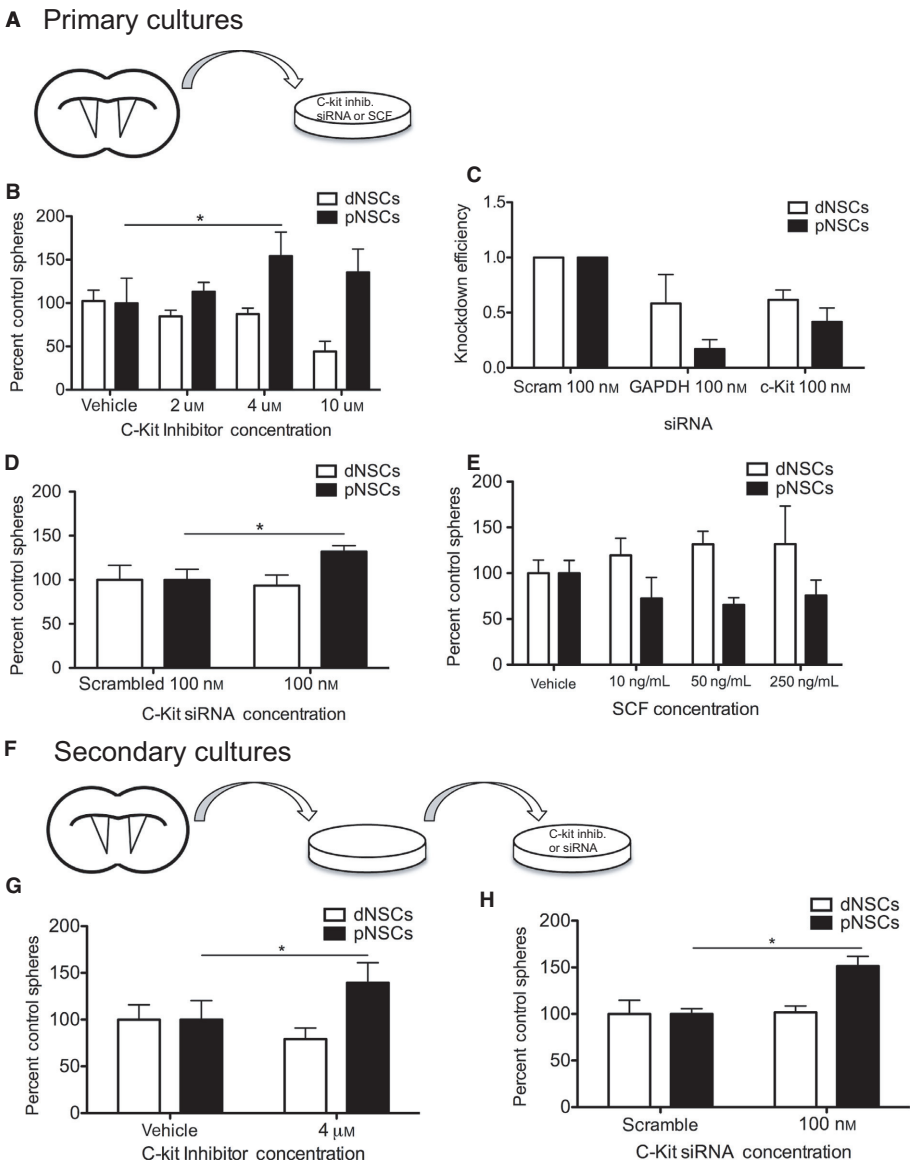

FIG. 4. Inhibition of C-Kit signalling increased pup-derived pNSC neurosphere formation. (A) Cultures of pNSCs and dNSCs were cultured with C-Kit inhibitor and Kit siRNA. (B) Addition of C-Kit inhibitor to primary cultures increased pNSCs and depleted dNSCs at increasing concentrations, causing a significant increase in pNSCs over dNSCs (two-way ANOVA $F_{3,24} = 3.55$, $P = 0.03$, $n = 4$). (C) Efficiency of GAPDH (positive control) and Kit siRNA knockdown by qPCR (two-way ANOVA $F_{2,13} = 15.23$, $P = 0.001$, $n = 3$). (D) An siRNA specific to C-Kit similarly increased pNSC spheres in primary culture significantly over scramble control without affecting dNSC-derived neurospheres (two-way ANOVA $F_{1,12} = 7.91$, $P = 0.02$, $n = 4$). (E) Addition of the C-Kit ligand SCF had a significant effect on the interaction of pNSCs vs. dNSCs at increasing doses (two-way ANOVA $F_{5,24} = 3.00$, $P = 0.03$, $n = 3$). (F) To test stem/progenitor-specific effects, primary cultures were passaged into secondary cultures in the presence of C-Kit inhibitor. (G) Addition of C-Kit inhibitor to secondary cultures of passaged pNSCs and dNSCs similarly increased pNSCs and depleted dNSCs, leading to significantly increased pNSCs over dNSCs (two-way ANOVA $F_{1,11} = 4.96$, $P = 0.05$, $n = 4$). (H) C-kit siRNA significantly increased secondary pNSC neurosphere formation without an effect on dNSCs (two-way ANOVA $F_{1,8} = 6.26$, $P = 0.05$, $n = 3$). $^*P \leq 0.05$.

treated spheres were 61.8 ± 2.2 μm), suggesting that proliferation was not responsible for the increase in sphere numbers. Together, these data suggest that C-Kit inhibition directly targets pup-derived pNSCs over dNSCs.

ErbB2 signalling has also been implicated as a requirement for pNSC proliferation (DeVeale *et al.*, 2014). We investigated whether ErbB2 inhibition depleted pup-derived pNSCs (Fig. 5A), similar to its effect on ESC-derived primitive neurospheres (DeVeale *et al.*, 2014). At high concentrations (13 μM) ErbB2 inhibition completely abolished pNSC- and dNSC-derived neurospheres (data not shown), as previously reported (DeVeale *et al.*, 2014). At lower concentrations, ErbB2 inhibition abolished dNSCs but not pup-derived pNSC neurospheres, which were significantly increased over dNSCs but not over vehicle-treated pNSC neurospheres (Fig. 5B). Although adding the ErbB2 inhibitor *in vitro* did not significantly increase pNSC neurospheres over control, we tested whether the ErbB2 siRNA increased dNSC or pNSC neurospheres, as it may have improved specificity compared to the pharmacological inhibitor. The ErbB2 siRNA knockdown efficiency was confirmed via qPCR to be 44% of control (Fig. 5C). ErbB2 siRNA attenuated dNSC neurosphere formation while increasing pNSC-derived neurospheres, resulting in a significant increase over a scramble siRNA control (Fig. 5D). To confirm that the ErbB2 inhibitor targeted the stem cell populations rather than niche cells in the dish, we added ErbB2 inhibitor to secondary cultures

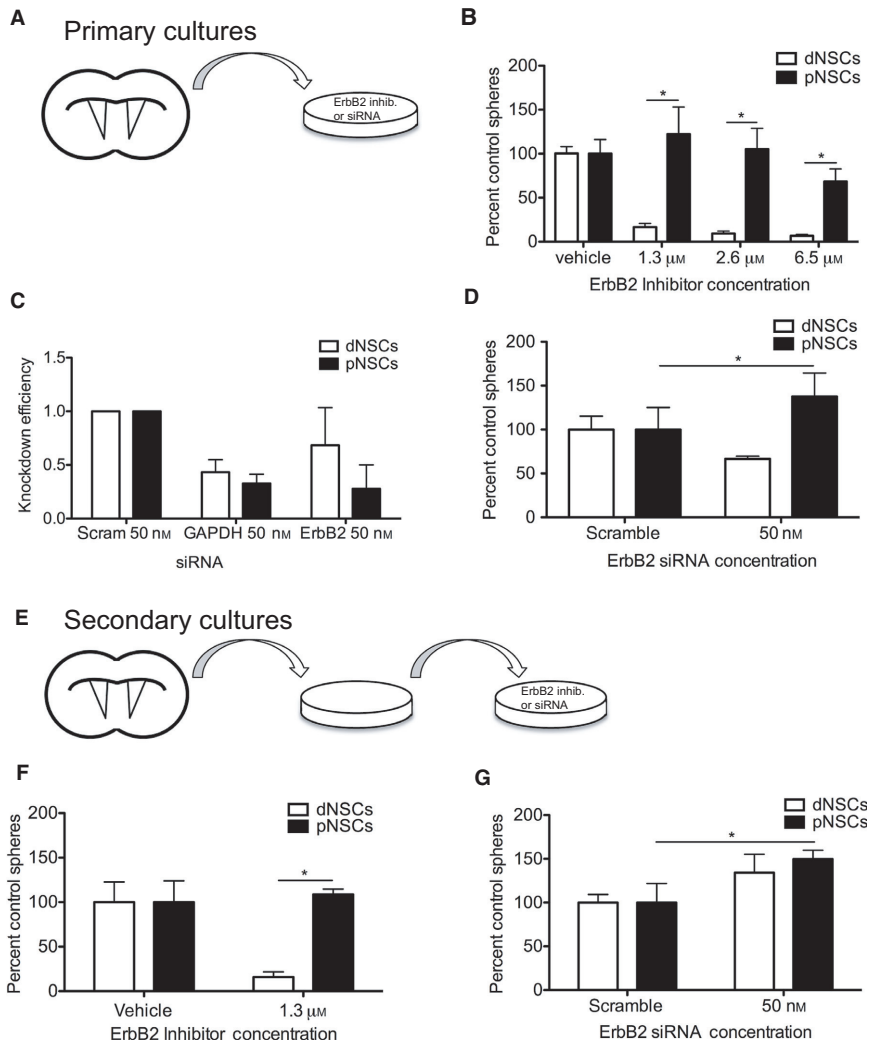

FIG. 5. ErbB2 inhibition increased pup-derived pNSC neurospheres. (A) Primary cultures of pNSCs and dNSCs were cultured with ErbB2 inhibitor and ErbB2 siRNA. (B) Addition of ErbB2 inhibitor to primary cultures attenuated dNSC neurosphere formation, while pNSC neurospheres were selectively increased at a low concentration (two-way ANOVA $F_{3,19} = 5.05$, $P = 0.01$, $n = 3$). (C) Efficiency of GAPDH (positive control) and ErbB2 siRNA knockdown by qPCR (two-way ANOVA $F_{2,14} = 8.45$, $P = 0.01$, $n = 3$). (D) ErbB2 siRNA had a similar effect in primary culture and decreased dNSCs while increasing pNSCs (two-way ANOVA $F_{1,12} = 7.03$, $P = 0.02$, $n = 4$). (E) To test stem/progenitor-specific effects, primary cultures were passaged into secondary cultures in the presence of ErbB2 inhibitor. (F) In secondary cultures of passaged pNSC and dNSC spheres, dNSCs spheres were severely attenuated with little effect on pNSCs, leading to a significant increase in pNSCs over dNSCs (two-way ANOVA $F_{1,9} = 8.69$, $P = 0.02$, $n = 3$). (G) ErbB2 siRNA increased both secondary dNSC and pNSC neurosphere formation (two-way ANOVA $F_{1,10} = 6.02$, $P = 0.03$, $n = 4$). $^*P \leq 0.05$.

(Fig. 5E). ErbB2 inhibitor in secondary cultures severely depleted dNSC neurospheres and significantly increased pNSC- over dNSC-derived neurospheres, but not compared to vehicle control, similar to its effect on primary culture (Fig. 5F). ErbB2 siRNA significantly increased the pNSC neurospheres compared to control conditions, but interestingly dNSC neurospheres were not depleted in the secondary culture (Fig. 5G). Neurosphere sphere size was not affected by exposure to ErbB2 siRNA (control pNSC neurospheres were 61.5 ± 1.0 μm whereas ErbB2 siRNA-treated spheres were 66.1 ± 4.3 μm), suggesting that proliferation was not responsible for the increase in sphere numbers. These *in vitro* experiments confirm that ErbB2 has cell-type-specific effects on pNSCs and dNSCs.

Cell surface proteins that increased pup-derived pNSCs targeted adult pNSCs in vivo

To determine whether the cell surface markers that we tested on pup-derived neurospheres *in vitro* were expressed *in vivo*, we prepared wholemounts of the pup periventricular region from Oct4-GFP mice. Immunostaining identified Oct4$^+$ cells that co-express C-kit and ErbB2 on the cell surface (Fig. 6A). After identifying expression in pup pNSCs *in vivo*, we delivered the C-Kit and ErbB2 inhibitors directly into the lateral ventricles of adult mice via cannula connected to a micro-osmotic pump to determine whether these inhibitors similarly increased adult-derived pNSC neurospheres (Fig. 6B). Mice received drug infusions over 3 days and were dissected immediately thereafter for a neurosphere assay to determine the effects of C-Kit or ErbB2 inhibition on adult pNSCs and dNSCs *in vivo*. When quantified with the neurosphere assay to test for the effect of the inhibitors on cells *in vivo*, direct infusion of the C-Kit inhibitor significantly increased pNSC-derived neurospheres to 288 ± 64% (mean ± SEM) of vehicle-infused control, without a significant effect on dNSCs. ErbB2 inhibitor infusion significantly increased pNSC-derived neurospheres to 358 ± 97% (mean ± SEM) of control, without affecting dNSCs (Fig. 6C). C-kit and ErbB2 inhibitors infused together significantly increased pNSC-

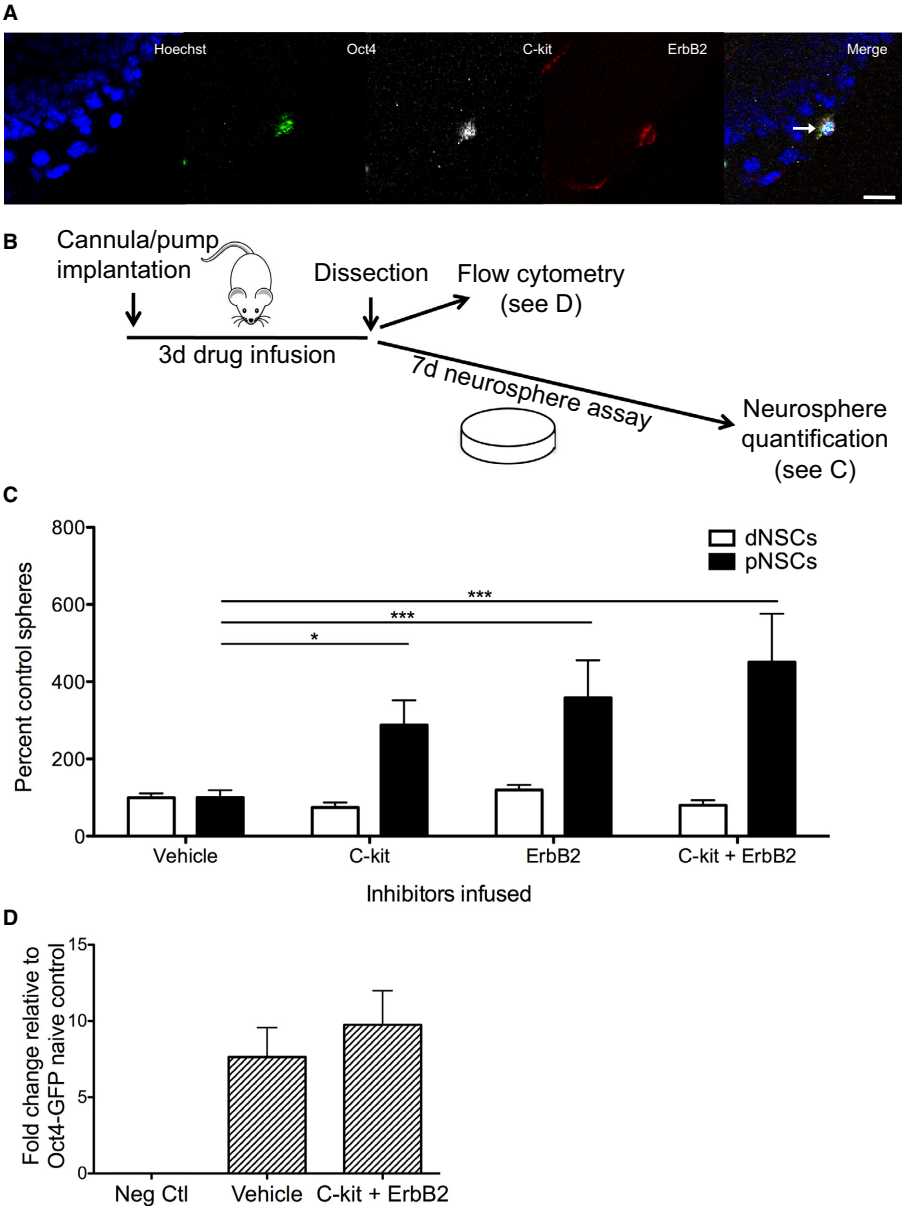

FIG. 6. C-Kit and ErbB2 are expressed on pNSCs *in vivo*. (A) Wholemount image of an Oct4$^+$ pNSC that co-expresses C-kit and ErbB2 from a pup mouse brain. Scale bar = 10 μm. (B) Pharmacological inhibitors were infused directly into the lateral ventricle of adult mice, and mice were dissected for either flow analysis to quantify the number of Oct4$^+$ cells or for quantification via the neurosphere assay. (D) C-Kit infusion, ErbB2 infusion and C-kit and ErbB2 combined infusion into the adult mouse brain significantly increased pNSC neurospheres relative to vehicle control without affecting dNSC number (two-way ANOVA $F_{3,35} = 5.63$ $P = 0.001$, $n = 8$–10). (C) Infusion of C-kit and ErbB2 inhibitors into the mouse brain did not increase the number of Oct4$^+$ cells by flow analysis. $^*P \leq 0.05$, $^{***}P \leq 0.001$.

derived neurospheres to 450 ± 125% (mean ± SEM) compared to control. However, this was not significantly increased over either inhibitor alone (Fig. 6C). The absence of an additive increase may result from a ceiling effect reached at the drug doses administered or a convergence at the molecular level downstream of the receptors, potentially via the PI3K/AKT pathway that is activated by both C-kit and ErbB2 (reviewed by Johnson, 2009). Flow analysis was performed on Oct4-GFP mice after drug infusion to determine whether this increase in neurosphere formation was due to pNSCs proliferating *in vivo*. C-kit and ErbB2 infusion did not increase the number of Oct4$^+$ cells relative to saline-infused controls (Fig. 6D), suggesting that the increase in pNSC neurospheres seen after inhibitor infusion *in vivo* is due to the drugs activating quiescent pNSCs that were already present *in vivo* rather than by inducing symmetric divisions to expand the population. This is similar to the siRNA transfection in culture where neither the C-kit nor the ErbB2 siRNAs changed neurosphere size, suggesting that proliferation of already active pNSCs was not affected. These data show that both ErbB2 and C-Kit are novel signalling pathways that can be targeted to induce activation of the pNSC population *in vivo*.

Discussion

pNSCs located in the periventricular region of the mouse brain are at the top of the NSC hierarchy (Tropepe *et al.*, 2001; Hitoshi *et al.*, 2004; Smukler *et al.*, 2006; Sachewsky *et al.*, 2014). Here we show that P7 pup-derived pNSCs are more numerous than adult pNSCs but otherwise comparable. P7-derived pNSCs self-renewed at the

same frequency, were multipotential and had similar gene expression by qPCR. Pup pNSCs were Oct4$^+$, SOX2$^+$ and LIF-R$^+$, similar to adult pNSCs (Sachewsky *et al.*, 2014), and were β-catenin$^+$. In addition, pup pNSC-derived neurospheres arose from the Oct4$^+$, GFAP$^-$, nestin^{mid} populations after FACS. The increased abundance of pup pNSCs makes them an ideal population to test C-kit and ErbB2 inhibition to activate adult pNSCs *in vivo*. We show that cell surface proteins identified on *in vitro* ESC-derived primitive neurospheres and validated using pup-derived NSCs modelled pNSCs in the adult mouse brain.

We targeted endogenous pNSCs to develop strategies to activate the earliest cell in the NSC lineage. pNSCs give rise to dNSCs and are *Oct4*-expressing, as shown by qPCR, immunohistochemistry, antibiotic resistance conferred by the endogenous *Oct4* promoter, flow cytometry sorting and the ability to integrate into the inner cell mass in a morula aggregation experiment (Sachewsky *et al.*, 2014). Expanding pNSCs at the top of the neural hierarchy could lead to exponential increases in dNSCs and downstream progeny. These data suggest that pNSCs have the potential to contribute to endogenous repair strategies. Infusion of the pharmacological inhibitors directly into the brains of adult mice induced an approximately three-fold increase in pNSC-derived neurospheres over vehicle-infused controls. dNSCs were not depleted when the drugs were delivered *in vivo*, suggesting that the niche influences the pharmacological inhibition or that niche-dependent signals on dNSCs were not overcome.

The three-fold increase in pNSC neurospheres observed when C-Kit inhibitor or ErbB2 inhibitor were infused *in vivo* without a proportionate increase in the number of Oct4$^+$ cells *in vivo* suggests that not all pNSCs have the ability to proliferate under baseline conditions and that pharmacological inhibition can activate pNSCs to proliferate when placed in culture. This activation in a restrictive environment may explain the larger effect observed after *in vivo* delivery vs. *in vitro* exposure where the cells have already been removed from their niche. In addition, pup pNSC neurospheres were not altered in size when exposed to the inhibitors *in vitro*, which supports the interpretation that C-Kit and ErbB2 inhibition do not induce proliferation of pNSCs, but rather may release pNSCs from quiescence that normally would not be able to proliferate to form a neurosphere and thus lead to an increase in the number of pNSC neurospheres.

We previously reported that 80 Oct4$^+$ cells can be isolated from the adult mouse periventricular region with flow, but only five pNSC neurospheres form per adult brain (Sachewsky *et al.*, 2014). Therefore, we suggest that the remaining Oct4$^+$ cells predicted by flow cytometry are quiescent pNSCs that do not form neurospheres in standard culture conditions. Others have reported that C-Kit ligands are overexpressed following brain injury (Sun *et al.*, 2006), and ErbB2 signalling maintains cells in an undifferentiated state (Schmid *et al.*, 2003), which is consistent with their inhibition modulating endogenous NSC activation. These studies suggest that the balance of cell surface signalling may regulate NSC quiescence and activation, and overcoming quiescence could enable pNSCs to contribute to endogenous repair. Our data suggest that C-Kit and ErbB2 signalling might act as barriers to pNSC activation after injury, and hold promise as valuable targets to modulate NSC-induced regeneration.

C-Kit is expressed at high levels in the neural tube and ventricular regions during embryonic development and its expression continues in the periventricular region, olfactory bulbs, cerebral cortex and hippocampus in the adult mouse brain (Keshet *et al.*, 1991; Motro *et al.*, 1991; Jin *et al.*, 2002). We did not detect a change in neurosphere size in the presence of C-Kit siRNA, suggesting that C-Kit does not exert a proliferation effect on the progeny of pNSCs, and our previous work observed that C-Kit does not exert a survival effect (DeVeale *et al.*, 2014). This previous work suggested that C-Kit inhibition might repress a quiescence-inducing signal (DeVeale *et al.*, 2014), which is consistent with the present report where we observed increased pNSC proliferative effects after the inhibitors were delivered *in vivo*, where we predict that pNSCs are predominantly quiescent under baseline conditions (our unpubl. data).

ErbB2 inhibition reduced proliferative capacity of ESC-derived pNSC neurospheres when used at a high dose (13 μM) (DeVeale *et al.*, 2014). We observed that low-dose (1.3 μM) ErbB2 inhibition increased pup-derived pNSC neurospheres when delivered *in vitro* and increased adult-derived pNSC neurospheres approximately three-fold when delivered *in vivo*, without affecting dNSCs *in vivo*. ErbB2 expression is present in the brain at E13 and becomes restricted during development so that by postnatal day 7 it is predominantly restricted to the periventricular regions and persists into the adult (Fox & Kornblum, 2005). Reduced ErbB2 activity led to differentiation of E9.5-derived radial glial cells into astrocytes in culture (Schmid *et al.*, 2003), which is consistent with the loss of dNSCs in our culture experiments. The loss of dNSCs *in vitro* but not *in vivo* in response to ErbB2 inhibition suggests that the drug can target pNSCs in the brain without a detrimental effect on dNSCs. Conversely, we found that pNSCs were not lost or induced to differentiate, but activated to form more neurospheres. This supports ErbB2 inhibition as a potentially useful mechanism to stimulate endogenous regeneration by activating the upstream pNSC, leading to a greater expansion of the downstream dNSCs and improved ability to generate neuronal and glial cells lost to injury.

The cell surface receptor inhibitors add to the differences between the two NSC populations. pNSCs and dNSCs are both multipotential, but vastly differ in frequency, differentiation profiles, and gene and protein expression. pNSCs are Oct4$^+$, Sox2$^+$, LIF-R$^+$, β-catenin$^+$ and have higher expression of stem cell markers and lower expression of neural commitment markers than dNSCs, regardless of age of origin. Whether derived from postnatal day 7 or adult brain, pNSCs self renewed at a low frequency, suggesting that they undergo asymmetric division given that a singly passaged neurosphere gave rise to only one new neurosphere, whereas dNSCs expand upon passaging suggesting symmetric expansion divisions (Reynolds & Weiss, 1992; Morshead *et al.*, 1994; Chiasson *et al.*, 1999). pNSCs generated fewer astrocytes than dNSCs, more oligodendrocytes from the pup brain and more neurons from the adult brain compared to dNSCs. Together, these findings support the suggestion that pNSCs and dNSCs are distinct cell populations present in the developing and adult mouse brain, with pNSCs able to generate dNSCs as previously reported (Sachewsky *et al.*, 2014).

Many neurodegenerative diseases and injuries lead to neuron loss and demyelination. pNSCs generate equal proportions of neurons, astrocytes and oligodendrocytes when differentiated in culture, unlike dNSCs, which generate predominantly astrocytes *in vitro*. The differentiation profiles suggest that pNSCs might be the preferential population to target to generate non-astrocyte cell types if pNSCs exhibit this characteristic *in vivo.* In this study, we demonstrate that a short infusion of pharmacological inhibitors activates pNSCs, without affecting dNSCs *in vivo*, and this could be used in conjunction with a cue for differentiation to produce a two-step strategy in the future. Demyelinating diseases would benefit from the activation of an upstream NSC with the capability of producing oligodendrocytes in the brain.

We compared pup and adult pNSCs and concluded that despite the large difference in abundance, the populations are analogous. The perinatal peak in active pNSCs capable of proliferation to form neurospheres may imply that pNSCs have a specific role in postnatal development, and the increased propensity to differentiate into oligodendrocytes in culture suggests that pNSCs may contribute to the wave of oligodendrogenesis postnatally. We performed flow cytometry for Oct4-GFP primary periventricular cells and quantified 0.08% of P7 pup-derived cells as $Oct4^+$, similar to the number of $Oct4^+$ cells reported in the adult periventricular region (Sachewsky *et al.*, 2014). This observation suggests two opposing hypotheses. First, the increased number of P7 pup pNSC-derived neurospheres may arise from a mixed population of stem and progenitors that self-renew only perinatally (Seaberg *et al.*, 2005; Clarke & van der Kooy, 2011). Second, all pup pNSCs survive but become predominantly quiescent during development, and thus persist into the adult, although most do not generate neurospheres in our assay. These hypotheses could explain the consistent number of $Oct4^+$ cells but substantial decrease in pNSC-derived neurospheres in our adult cell cultures. That C-kit and ErbB2 inhibitor infusion did not affect the number of $Oct4^+$ cells but did increase the number of neurospheres also suggests there may be quiescent pNSCs not forming neurospheres unless activated. A long-term lineage tracing experiment with an inducible *Oct4* labelling system initiated immediately after birth might help elucidate pup pNSC fates.

While the fate of the expanded pup pNSC population remains unclear in the adult brain, we suggest that these pNSCs are upstream of the recently reported quiescent (q)NSCs (Codega *et al.*, 2014), and pre-GEPCOT cells (Mich *et al.*, 2014). Pre-GEPCOT cells were reported to be upstream of GEPCOT cells, which are $Glast^{mid}EGFR^{high}PlexinB2^{high}CD24^{-/low}O4/PSA\text{-}NCAM^{-/low}Ter119/CD45^-$ (Mich *et al.*, 2014). pNSCs are the least abundant in the niche and are the only NSCs that are $Oct4^+$ and $GFAP^-$, and thus comprise a distinct cell population. Therefore, pNSCs are a valuable population to develop methods to target NSCs for endogenous regeneration.

Many cell surface markers were identified in the ESC-derived mass spectrometry-based screen (DeVeale *et al.*, 2014). We can continue to take advantage of the abundant pup pNSC population to screen for signalling molecules targeting adult pNSCs. This will contribute to the development of pharmacological tools to target and activate NSCs in the adult brain to aid in endogenous recovery in response to brain injury or disease.

Conflict of interest

The authors have no conflicts of interest to disclose.

Acknowledgements

We thank all the members of the van der Kooy lab for their contribution to the manuscript, Shreya Shukla for assistance with flow analysis, Dionne White for assistance with FACS and Brenda Coles for technical assistance. This work was funded by the Canadian Institutes of Health Research, NeuroDevNet and the Ontario Brain Institute.

Abbreviations

dNSC, definitive neural stem cell; E, embryonic; EGF, epidermal growth factor; ESC, embryonic stem cell; FGF, fibroblast growth factor; GFAP, glial fibrillary acidic protein; LIF, leukaemia inhibitory factor; pNSC, primitive neural stem cell; P, postnatal; SCF, stem cell factor.

References

Akamatsu, W., DeVeale, B., Okano, H., Cooney, A.J. & van der Kooy, D. (2009) Suppression of Oct4 by germ cell nuclear factor restricts pluripotency and promotes neural stem cell development in the early neural lineage. *J. Neurosci.*, **29**, 2113–2124.

Blom, T., Fox, H., Angers-Loustau, A., Peltonen, K., Kerosuo, L., Wartiovaara, K., Linja, M., Jänne, O.A., Kovanen, P., Haapasalo, H. & Nupponen, N.N. (2008) KIT overexpression induces proliferation in astrocytes in an imatinib-responsive manner and associates with proliferation index in gliomas. *Int. J. Cancer*, **123**, 793–800.

Chiasson, B.J., Tropepe, V., Morshead, C.M. & van der Kooy, D. (1999) Adult mammalian forebrain ependymal and subependymal cells demonstrate proliferative potential, but only subependymal cells have neural stem cell characteristics. *J. Neurosci.*, **19**, 4462–4471.

Clarke, L. & van der Kooy, D. (2011) The adult mouse dentate gyrus contains populations of committed progenitor cells that are distinct from subependymal zone neural stem cells. *Stem Cells*, **9**, 1448–58.

Codega, P., Silva-Vargas, V., Paul, A., Maldonado-Soto, A.R., Deleo, A.M., Pastrana, E. & Doetsch, F. (2014) Prospective identification and purification of quiescent adult neural stem cells from their in vivo niche. *Neuron*, **82**, 545–559.

Coles-Takabe, B.L.K., Brain, I., Purpura, K.A., Karpowicz, P., Zandstra, P.W., Morshead, C.M. & van der Kooy, D. (2008) Don't look: growing clonal versus nonclonal neural stem cell colonies. *Stem Cells*, **26**, 2938–2944.

DeVeale, B., Bausch-Fluck, D., Seaberg, R., Runciman, S., Akbarian, V., Karpowicz, P., Yoon, C., Song, H., Leeder, R., Zandstra, P.W., Wollscheid, B. & van der Kooy, D. (2014) Surfaceome profiling reveals regulators of neural stem cell function. *Stem Cells*, **32**, 258–268.

Doetsch, F., Caillé, I., Lim, D.A., García-Verdugo, J.M. & Alvarez-Buylla, A. (1999) Subventricular zone astrocytes are neural stem cells in the adult mammalian brain. *Cell*, **97**, 703–716.

Erlandsson, A., Larsson, J. & Forsberg-Nilsson, K. (2004) Stem cell factor is a chemoattractant and a survival factor for CNS stem cells. *Exp. Cell Res.*, **301**, 201–210.

Fox, I.J. & Kornblum, H.I. (2005) Developmental profile of ErbB receptors in murine central nervous system: implications for functional interactions. *J. Neurosci. Res.*, **79**, 584–597.

Gilyarov, A.V. (2008) Nestin in central nervous system cells. *Neurosci. Behav. Physiol.*, **38**, 165–169.

Hitoshi, S., Seaberg, R.M., Koscik, C., Alexson, T., Kusunoki, S., Kanazawa, I., Tsuji, S. & van der Kooy, D. (2004) Primitive neural stem cells from the mammalian epiblast differentiate to definitive neural stem cells under the control of Notch signaling. *Gene. Dev.*, **18**, 1806–1811.

Jin, K., Mao, X.O., Sun, Y., Xie, L. & Greenberg, D.A. (2002) Stem cell factor stimulates neurogenesis in vitro and in vivo. *J. Clin. Invest.*, **110**, 311–319.

Johnson, L.N. (2009) Protein kinase inhibitors: contributions from structure to clinical compounds. *Q. Rev. Biophys.*, **42**, 1–40.

Julian, L.M., Vandenbosch, R., Pakenham, C.A., Andrusiak, M.G., Nguyen, A.P., McClellan, K.A., Svoboda, D.S., Lagace, D.C., Park, D.S., Leone, G., Blais, A. & Slack, R.S. (2013) Opposing regulation of Sox2 by cell-cycle effectors E2f3a and E2f3b in neural stem cells. *Cell Stem Cell*, **12**, 440–452.

Keshet, E., Lyman, S.D., Williams, D.E., Anderson, D.M., Jenkins, N.A., Copeland, N.G. & Parada, L.F. (1991) Embryonic RNA expression patterns of the c-kit receptor and its cognate ligand suggest multiple functional roles in mouse development. *EMBO J.*, **10**, 2425–2435.

Mich, J.K., Signer, R.A., Nakada, D., Pineda, A., Burgess, R.J., Vue, T.Y., Johnson, J.E. & Morrison, S.J. (2014) Prospective identification of functionally distinct stem cells and neurosphere-initiating cells in adult mouse forebrain. *Elife*, **3**, e02669.

Mignone, J.L., Kukekov, V., Chiang, A.S., Steindler, D. & Enikolopov, G. (2004) Neural stem and progenitor cells in nestin-GFP transgenic mice. *J. Comp. Neurol.*, **469**, 311–324.

Miller, F.D. & Kaplan, D.R. (2012) Mobilizing endogenous stem cells for repair and regeneration: are we there yet? *Cell Stem Cell*, **10**, 650–652.

Mirzadeh, Z., Merkle, F.T., Soriano-Navarro, M., Garcia-Verdugo, J.M. & Alvarez-Buylla, A. (2008) Neural stem cells confer unique pinwheel architecture to the ventricular surface in neurogenic regions of the adult brain. *Cell Stem Cell*, **3**, 265–278.

Morshead, C.M., Reynolds, B.A., Craig, C.G., McBurney, M.W., Staines, W.A., Morassutti, D., Weiss, S. & van der Kooy, D. (1994) Neural stem

cells in the adult mammalian forebrain: a relatively quiescent subpopulation of subependymal cells. *Neuron*, **13**, 1071–1082.

Morshead, C.M., Garcia, A.D., Sofroniew, M.V. & van der Kooy, D. (2003) The ablation of glial fibrillary acidic protein-positive cells from the adult central nervous system results in the loss of forebrain neural stem cells but not retinal stem cells. *Eur. J. Neurosci.*, **18**, 76–84.

Motro, B., van der Kooy, D., Rossant, J., Reith, A. & Bernstein, A. (1991) Contiguous patterns of c-kit and steel expression: analysis of mutations at the W and Sl loci. *Development*, **113**, 1207–1221.

Obermair, F.J., Fiorelli, R., Schroeter, A., Beyeler, S., Blatti, C., Zoerner, B. & Thallmair, M. (2010) A novel classification of quiescent and transit amplifying adult neural stem cells by surface and metabolic markers permits a defined simultaneous isolation. *Stem Cell Res.*, **5**, 131–143.

Reynolds, B.A. & Weiss, S. (1992) Generation of neurons and astrocytes from isolated cells of the adult mammalian central nervous system. *Science*, **255**, 1707–1710.

Sachewsky, N., Leeder, R., Xu, W., Rose, K., Yu, F., van der Kooy, D. & Morshead, C. (2014) Primitive neural stem cells in the adult mammalian brain give rise to GFAP-expressing neural stem cells. *Stem Cell Reports*, **2**, 810–824.

Sauvageot, C.M. & Stiles, C.D. (2002) Molecular mechanisms controlling cortical gliogenesis. *Curr. Opin. Neurobiol.*, **12**, 244–249.

Schmid, R.S., McGrath, B., Berechid, B.E., Boyles, B., Marchionni, M., Sestan, N. & Anton, E.S. (2003) Neuregulin 1-erbB2 signaling is required for the establishment of radial glia and their transformation into astrocytes in cerebral cortex. *Proc. Natl. Acad. Sci. USA*, **100**, 4251–4256.

Seaberg, R.M., Smukler, S.R. & van der Kooy, D. (2005) Intrinsic differences distinguish transiently neurogenic progenitors from neural stem cells in the early postnatal brain. *Dev. Biol.*, **278**, 71–85.

Smukler, S.R., Runciman, S.B., Xu, S. & van der Kooy, D. (2006) Embryonic stem cells assume a primitive neural stem cell fate in the absence of extrinsic influences. *J. Cell Biol.*, **172**, 79–90.

Sun, L., Hui, A.-M., Su, Q., Vortmeyer, A., Kotliarov, Y., Pastorino, S., Passaniti, A., Menon, J., Walling, J., Bailey, R., Rosenblum, M., Mikkelsen, T. & Fine, H.A. (2006) Neuronal and glioma-derived stem cell factor induces angiogenesis within the brain. *Cancer Cell*, **9**, 287–300.

Surzenko, N., Crowl, T., Bachleda, A., Langer, L. & Pevny, L. (2013) SOX2 maintains the quiescent progenitor cell state of postnatal retinal Muller glia. *Development*, **140**, 1445–1456.

Tropepe, V., Sibilia, M., Ciruna, B.G., Rossant, J., Wagner, E.F. & van der Kooy, D. (1999) Distinct neural stem cells proliferate in response to EGF and FGF in the developing mouse telencephalon. *Dev. Biol.*, **208**, 166–188.

Tropepe, V., Hitoshi, S., Sirard, C., Mak, T.W., Rossant, J. & van der Kooy, D. (2001) Direct neural fate specification from embryonic stem cells: a primitive mammalian neural stem cell stage acquired through a default mechanism. *Neuron*, **30**, 65–78.

Viswanathan, S., Benatar, T., Mileikovsky, M., Lauffenburger, D.A., Nagy, A. & Zandstra, P.W. (2003) Supplementation-dependent differences in the rates of embryonic stem cell self-renewal, differentiation, and apoptosis. *Biotechnol. Bioeng.*, **84**, 505–517.

Yarden, Y. & Sliwkowski, M.X. (2001) Untangling the ErbB signaling network. *Nat. Rev. Mol. Cell Bio.*, **2**, 127–137.